

Point defect concentrations in metastable Fe-C alloys

Clemens J. Först,^{1,2} Jan Slycke,³ Krystyn J. Van Vliet,^{2,*} and Sidney Yip^{1,2}

¹ *Department of Nuclear Science and Engineering,
Massachusetts Institute of Technology, Cambridge, Massachusetts 02139, USA*

² *Department of Materials Science and Engineering,
Massachusetts Institute of Technology, Cambridge, Massachusetts 02139, USA and*

³ *Department of Materials Science, SKF Engineering Research Centre,
P.O. Box 2350, 3430 DT Nieuwegein, The Netherlands*

(Dated: September 15, 2018)

Point defect species and concentrations in metastable Fe-C alloys are determined using density functional theory and a constrained free-energy functional. Carbon interstitials dominate unless iron vacancies are in significant excess, whereas excess carbon causes greatly enhanced vacancy concentration. Our predictions are amenable to experimental verification; they provide a baseline for rationalizing complex microstructures known in hardened and tempered steels, and by extension other technological materials created by or subjected to extreme environments.

PACS numbers: 71.15.Mb, 71.15.Nc 67.40.Yv 61.72.Ji,

Many industrially significant alloys are intentionally processed as metastable microstructures comprising a supersaturation of crystal defects in various forms of aggregation [1, 2]. How the defects are distributed and in what local concentrations they exist are fundamental questions which are not yet resolved experimentally, yet it is this microstructural complexity that governs the performance of the material. Hardened steels are an important example where deformation behavior is intrinsically coupled to the lattice defects: in this case, a body-centered cubic (bcc) Fe matrix with carbon content in excess of equilibrium values for ferrite (solid solution of carbon in bcc Fe) and cementite (Fe_3C), as well as high dislocation density and supersaturation of vacancies [1]. While it is generally known that carbon binds strongly to crystal defects such as vacancies, what is lacking is a robust computational strategy capable of linking the fundamental physics of crystal defects and their energetics with quantitative, microscopic details of the defect microstructure as it evolves during processing and service.

In this work we determine the concentration of point defects and defect clusters in Fe-C alloys using an approach based on first-principles calculation of the formation energies of specific defects, and a free-energy formulation allowing either the carbon or the iron vacancy concentration to be out of equilibrium. We find that the vacancy concentration in the form of carbon-vacancy clusters increases dramatically in the presence of carbon due to strongly exothermic clustering reactions. Nevertheless, the concentrations of carbon-vacancy clusters remain orders of magnitude below the concentration of interstitial carbon. Only under the assumption of a significant supersaturation of vacancies will carbon-vacancy clusters begin to dominate the defect spectrum, in accord with experimental observation of dominant carbon-vacancy clusters in irradiated bcc-Fe alloys [3]. Ab-initio results on the structure and energetics of vacancies, self-interstitials and carbon interstitials in bcc-Fe have been

reported previously [4, 5], as well as the interaction of one and two C interstitials with the Fe vacancies [6]. Our results at 0 K are in close agreement with cluster formation energies reported previously [6]. Additionally, we have considered clusters with higher carbon contents and included di-vacancies in our considerations.

The supersaturation of carbon in such alloys has been established through several experimental approaches, although the degree of supersaturation in the bcc-Fe matrix ranges from 0.3 at.% C upon 400°C annealing [7] to up to 5 at.% C in volumes including ferritic grain boundaries [8, 9]. While experiments can quantify local carbon concentrations (e.g., three-dimensional atom probe [8]) or determine the carbon-vacancy binding energy [10] (a value of 0.85 eV was reported by positron annihilation measurements [1]), it is not yet feasible to measure the relative concentrations and specific structures of C-vacancy clusters in bcc-Fe during thermal processing. The most likely C-related defects are: (1) simple interstitial supersaturation [7]; (2) co-association with vacancies as inferred from reduced vacancy diffusion [1] and carbon segregation to vacancy rich regions [3]; (3) direct observation of elevated carbon concentration up to 8 at.% near dislocation cores [8]; (4) up to 6.6 at.% at grain boundaries [7, 8].

We have performed a set of total energy calculations on the interaction of carbon with single and double vacancies and applied the results in a statistical mechanics model to obtain parameter-free estimates of the concentration of point defects in various structural configurations in the bcc-Fe matrix. We employed density functional theory (DFT) [11, 12, 13] using Blöchl's projector augmented wave method [14, 15] as implemented in the VASP code [16, 17] with a plane-wave cutoff of 400 eV. The calculations were performed in 128-atom supercells with the theoretical lattice constant of 2.83 Å, using a k-mesh of $2 \times 2 \times 2$ and a Methfessel Paxton Fermi-surface smearing parameter of 0.05 eV [18]. No symmetry con-

straints were imposed. Screening calculations and vibrational frequency calculations were carried out in 54-atom supercells. The geometry optimization was terminated with a force cutoff of 5 meV/Å. All calculations included spin polarization, starting with a ferromagnetic charge density. Because a wide variety of different bulk and defect structures are considered, we anticipate an error of 0.1–0.2 eV for the defect formation energies. At the target temperature of 160°C, where the body centered tetragonal phase transforms to bcc, this implies error in species concentration of one to two orders of magnitude. However, the overall conclusions regarding the dominant defect concentrations are not found to be affected by this level of uncertainty.

Table I summarizes the formation energies of the defects and defect clusters under consideration,

$$E^{\text{form}}(T, \mu_{\text{Fe}}, \mu_{\text{C}}) = E^{\text{D}}(T) - E^0(T) - \mu_{\text{Fe}} \cdot \Delta n_{\text{Fe}} - \mu_{\text{C}} \cdot \Delta n_{\text{C}}, \quad (1)$$

where $E^{\text{D}}(T)$ and $E^0(T)$ denote the DFT energies of the supercells with and without defects present, and μ_X and Δn_X are the chemical potential of species X and the difference in atom number between the two supercells. Temperature dependence is taken into account through configurational and vibrational free energy contributions, the latter being calculated using the dynamical matrix of all atoms affected by the defect formation. To approximate the vibrational free energy we consider each atom as a three-dimensional harmonic oscillator with force-constants derived from ab-initio total energy calculations. The vibrational frequencies of carbon are found to be strongly dependent on the defect geometry, varying between 7 and 34 THz. Variation of the frequencies of Fe atoms in the vicinity of a (double-) vacancy with respect to the bulk value is less than 3 THz and is therefore neglected. The vibrational contributions to the formation energies can amount to 0.2 eV at 160°C.

Table I shows the most stable configuration for a given stoichiometry. While there are different ways to arrange a given number of C atoms around an Fe (double-)vacancy, we find that these typically have very different formation energies. A more extensive list of energetics of one and two carbon atoms near a single vacancy can be found in Ref. [6]. Here we regard structures with formation energies within 0.1 eV (our approximate error) to be degenerate. Structures with energies greater than 0.3 eV relative to the lowest-energy configuration are not considered.

Figure 1 shows the stable geometries for an Fe vacancy surrounded by up to six carbon atoms. In the case of di-vacancies, we need to distinguish between two possible orientations [100] and [111], which are energetically practically degenerate in the carbon-free state (compare Fig. 2 and Table I). Around a [111] vacancy there are two

TABLE I: Formation energies for the different defect stoichiometries at 160°C. The chemical potentials $\mu_{\text{Fe/C}}$ (compare Eqn. 1) are chosen to represent thermal equilibrium of bulk Fe and Fe₃C. X_I and X_V refer to an interstitial and a vacancy of species X , respectively. Parentheses (...) denote a defect cluster. The crystallographic directions [...] refer to the orientation of the iron double-vacancies.

defect species	E^{form} [eV]	defect species	E^{form} [eV]
C_I octahedral	0.58	$(2Fe_V + 2C)$ [100]	3.31
Fe_V	2.02	$(2Fe_V + 3C)$ [100]	3.21
Fe_I	3.91	$(2Fe_V + 4C)$ [100]	2.77
$(Fe_V + 1C)$	1.96	$(2Fe_V + 5C)$ [100]	3.23
$(Fe_V + 2C)$	1.53	$(2Fe_V + 6C)$ [100]	3.74
$(Fe_V + 3C)$	1.98	$(2Fe_V + 7C)$ [100]	5.78
$(Fe_V + 4C)$	3.03	$(2Fe_V + 1C)$ [111]	3.66
$(Fe_V + 5C)$	6.58	$(2Fe_V + 2C)$ [111]	3.06
$(Fe_V + 6C)$	13.48	$(2Fe_V + 3C)$ [111]	2.91
$(2Fe_V)$ [100]	3.83	$(2Fe_V + 4C)$ [111]	2.43
$(2Fe_V)$ [111]	3.85	$(2Fe_V + 5C)$ [111]	3.50
$(2Fe_V + 1C)$ [100]	3.49	$(2Fe_V + 6C)$ [111]	4.76

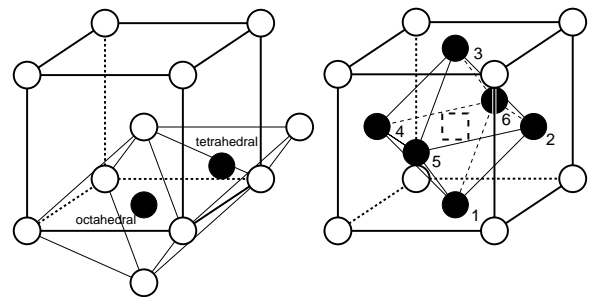


FIG. 1: Atomic structure of C interstitials and C-vacancy clusters in bcc-Fe. Fe atoms in open circles, carbon atoms filled circles. Left panel: octahedral and tetrahedral carbon interstitials; right panel: position of carbon atoms around a vacancy. A carbon-vacancy cluster with n carbon atoms contains the C atoms with labels from 1 to n .

types of adsorption sites: those with one of the six coordinating Fe atoms missing (shaded sides in Fig. 2) and those with two missing coordinating atoms. We find that configurations with two missing coordinating Fe atoms are energetically unfavorable. Otherwise, the stable carbon geometries are analogous to that of the isolated vacancy. In the case of the [100] oriented di-vacancy, the configuration of a single carbon atom situated between the two vacancies is most favorable; however, this preference does not hold for pairs and triplets of C atoms. From screening a wide variety of C geometries, including chains and tetrahedra connecting two vacancies, no new, low-energy carbon configurations are found.

The formation of a C-vacancy cluster by combining a vacancy with n carbon interstitials,

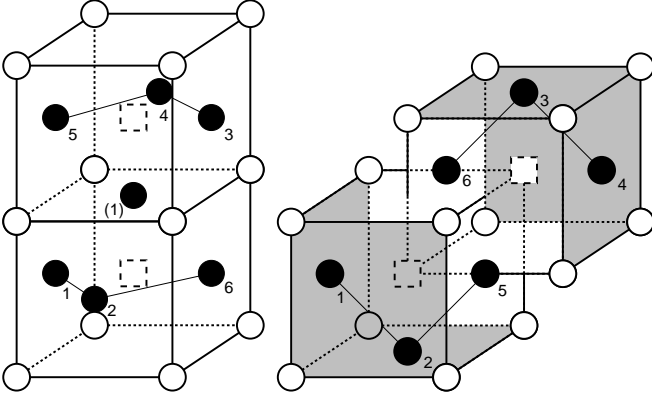


FIG. 2: Atomic structure of C-double vacancy clusters oriented in [100] (left panel) and [111] (right panel) directions. Refer to Fig. 1 for labeling. In case of the [100] vacancy, the position '(1)' is only occupied if there is a single C atom.



is seen to give a negative reaction enthalpy ΔH for $n \leq 4$ (Table I). The same is also predicted for two single vacancies/C-vacancy clusters forming a di-vacancy/C-di-vacancy cluster (e.g., $2(Fe_V + 2C) \rightarrow (2Fe_V + 4C)$ [111] with $\Delta H = -0.6$ eV). However, one should note that the mass-action law for a clustering reaction such as $X + X \rightarrow X_2$ relates the concentration of the cluster c_{X_2} to the square of the concentration of the individual defects, $(c_X)^2$. Thus the defect complex is the dominating species only if $\exp(-\frac{\Delta H}{k_B T})$ is larger than $1/c_X$. For typical defects in solids, c_X is often very small ($\ll 1$ ppm) and ΔH is on the order of -0.1 eV, so this condition is not necessarily fulfilled. Nonetheless, enthalpy provides a measure of “thermal stability” of a complex once it is formed, as in the case of vacancy agglomerates [1].

The equilibrium concentrations of defects c_i in a macroscopic crystal are given by minimizing the free energy $F(T, \mu_{Fe}, \mu_C)$ at given temperature T and chemical potentials μ_{Fe} and μ_C :

$$F(T, \mu_{Fe}, \mu_C) = \sum_{i=1}^M c_i E_i^{\text{form}}(T, \mu_{Fe}, \mu_C) + k_B T \sum_{i=1}^M \left[c_i \ln c_i + (1 - c_i) \ln(1 - c_i) \right], \quad (3)$$

where E^{form} is defined in Eqn. 1, M denotes the number of different defect species and c_i is the concentration of defect species i [19]. One obtains from Eqn. 3

$$c_i(T, \mu_{Fe}, \mu_C) = \frac{1}{\exp\left(\frac{E_i^{\text{form}}(T, \mu_{Fe}, \mu_C)}{k_B T}\right) + 1}. \quad (4)$$

The dependence on the two chemical potentials, which enters through the formation energies, can be turned into an explicit dependence on the total carbon and/or vacancy concentrations if we impose the respective constraints:

$$\sum_{i=1}^M c_i \cdot \Delta n_{V_a/C}^i = c_{V_a/C}^{\text{tot}}. \quad (5)$$

This is useful for performing calculations under physically motivated hypotheses.

As discussed above, carbon and vacancy concentrations in realistic microstructures of Fe-C alloys need to be treated as nonequilibrium. To make the calculations tractable we consider two alternative hypotheses under the condition of partial thermodynamic equilibrium. That is, we have thermal equilibrium for one species (e.g., Fe) and non-equilibrium for the other (e.g., C), thus reducing the problem to a study of the effects of the concentration of the non-equilibrium species. In hypothesis (1) the carbon concentration is not in equilibrium with the Fe_3C/Fe system, whereas Fe is assumed to be in equilibrium with bulk Fe. This scenario is motivated by the experimental observation that carbide precipitation is kinetically hindered and requires tempering at elevated temperatures [7]. It is also implied that the Fe matrix remains substantially undistorted. In hypothesis (2) the vacancy concentration is assumed to be non-equilibrium, whereas carbon is assumed to equilibrate with the bulk Fe/Fe_3C system. This reflects the anticipated processing conditions for hardening of Fe-C alloys; in the course of martensitic transformation, large plastic strain leads to high intrinsic defect concentrations, with vacancies binding strongly to carbon interstitials. Due to the increased diffusion barriers associated with carbon-vacancy clusters [1] and the absence of a comparable number of Fe interstitials (high formation energies), it is likely that a significant vacancy concentration is effectively frozen in. These two hypotheses represent extreme scenarios; any intermediate situation can also be studied using the present data.

Figure 3 shows the consequences of hypothesis (1), the variation of dominant defect species concentrations with the total carbon concentration. These results are obtained by taking the chemical potential μ_{Fe} to be the bulk Fe value, while μ_C is given by the total carbon concentration (Eqn. 5). We observe that the presence of carbon in the matrix can cause the vacancy concentration (including carbon-vacancy clusters) to increase by 15 orders of magnitude relative to the intrinsic vacancy concentration (Fe_V) at a total carbon concentration of 1 at.%. Comparable increases in vacancy concentration have been reported in the presence of a different impurity atom, hydrogen [21, 22]. We also note that the concentration of carbon-free di-vacancies is negligible.

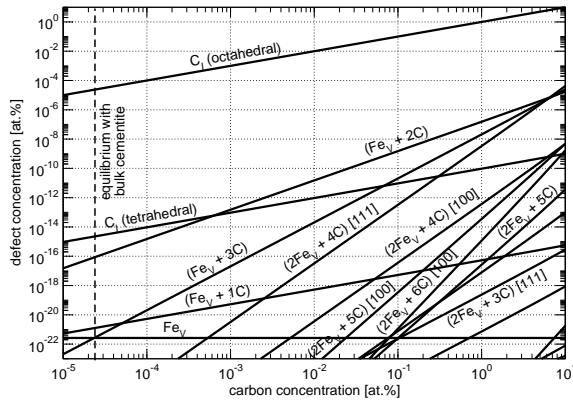


FIG. 3: Defect concentrations in a bcc-Fe matrix as a function of the total carbon concentration at 160°C. Labeling as in Table I. The vertical dashed line marks thermal equilibrium with bulk cementite. Note that that small precipitates are expected to have less favorable energetics in terms of atomic and magnetic structure, which may shift the equilibrium carbon concentration to higher values.

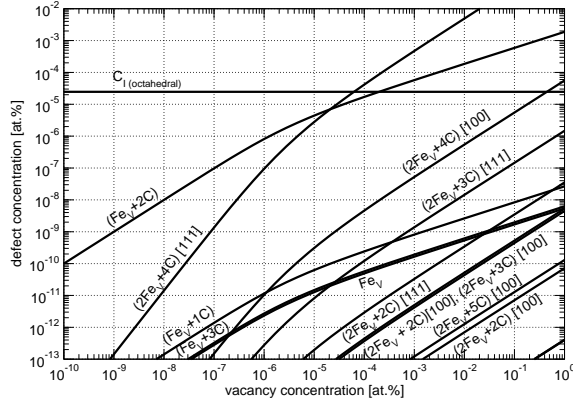


FIG. 4: Defect concentrations in a bcc-Fe matrix as a function of the total vacancy concentration at 160°C.

Figure 4 shows the defect concentration variation with total iron vacancy concentration under hypothesis (2). In this case μ_C is fixed at the reference value, the co-existence of Fe_3C and bulk Fe. We observe that the number of carbon atoms associated with vacancies exceeds the number of carbon interstitials only when the vacancy concentrations are larger than 10^{-4} at.%, which corresponds to a typical equilibrium vacancy concentration near the melting point [20]. This correlates with the experimental finding that C-vacancy clusters have been observed to be the dominant carbon-species in irradiated samples [3], which cannot be explained under the assumption of an equilibrated vacancy concentration (hypothesis (1)).

In conclusion, our work provides the first quantitative assessment of the interplay of different defect species in Fe-C alloys. We predict defect phase diagrams as a function of total carbon and vacancy concentrations, results

which are amenable to experimental verification. As a computational framework for addressing microstructure complexity, our approach should be applicable to other advanced technological materials subject to extreme environmental conditions.

The authors thank Alejandro Sanz and Fred Lucas for stimulating discussions, and acknowledge SKF for financial support. We have benefited from computational resources funded by NSF (IMR-0414849).

-
- [*] contact author: Krystyn J. Van Vliet (krystyn@mit.edu)
- [1] A. Vehanen, P. Hautojärvi, J. Hohannson, J. Yli-Kauppi and P. Moser, Phys. Rev. B **25**, 762 (1982).
 - [2] E. T. Ogawa, J. W. McPherson, J. A. Rosal, K. J. Dickerson, T.-C. Chiu, L. Y. Tsung, M. K. Jain, T. D. Bonifield, J. C. Ondrusek, and W. R. McKee, Proc. 40th Int. Reliability Physics Symp., p312 (2002).
 - [3] V.I. Lavrent'ev, A.D. Pogrebnnyak, A.D. Mikhalev, N.A. Pogrebnnyak, R. Shandrik, Z. Zecca and Y.V. Tsvintarnaya, Tech. Phys. Lett. **24**, 334 (1998)
 - [4] D. E. Jiang and E. A. Carter, Phys. Rev. B. **67**, 214103 (2003).
 - [5] C. Domain and C. S. Becquart, Phys. Rev. B. **65**, 24103 (2001).
 - [6] C. Domain, C. S. Becquart and J. Foct, Phys. Rev. B. **69**, 144112 (2004).
 - [7] S. Ohsaki, K. Hono, H. Hidaka and S. Takaki, Scripta.Met. **52**, 271 (2005).
 - [8] J. Wilde, A. Cerezo and G.D.W. Smith, Scripta Mater. **43**, 39 (2000).
 - [9] J. Slycke, SKF Engineering Research Centre, The Netherlands, unpublished work.
 - [10] B. T. A. McKee, W. Triftshuser, and A. T. Stewart, Phys. Rev. Lett. **28**, 358 (1972)
 - [11] P. Hohenberg and W. Kohn, Phys. Rev. **136**, B864 (1964).
 - [12] W. Kohn and L. J. Sham, Phys. Rev. **140**, A1133 (1965).
 - [13] J.P. Perdew, K. Burke, and M. Ernzerhof, Phys. Rev. Lett. **77**, 3865 (1996).
 - [14] P.E. Blöchl, Phys. Rev. B **50**, 17953 (1994).
 - [15] Peter E. Blöchl, Clemens J. Först and Johannes Schimpl, Bull. Mater. Sci. **26**, 33 (2003)
 - [16] G. Kresse and J. Furthmüller, Phys. Rev. B. **54**, 11169 (1996).
 - [17] G. Kresse and D. Joubert, Phys. Rev. B **59**, 1758 (1999).
 - [18] M. Methfessel and A.T. Paxton, Phys. Rev. B **40**, 3616 (1989)
 - [19] Note that we have assumed here that different defect species do not compete for sites in the bcc lattice, i.e. the number of iron sites available is large compared to the number of defects in the system. Considering a competition for defect sites the numerator of Eqn. 4 would be $(1 - \sum_{j \neq i} c_j)$.
 - [20] R.E. Reed-Hill and R. Abbaschian. Physical Metallurgy Principles. Boston: PWS Publishing Company (1994).
 - [21] V.G. Gavriljuk, V.N. Bugaev, Y.N. Petrov, A.V. Tarasenko and B.Z. Yanchitski, Scripta Mater. **34**, 903 (1996)
 - [22] R.B. McLellan and Z.R. Xu, Scripta Mater. **36**, 1201

(1997)